A New DC Offset Boostable Chaotic System with Multistability, Coexisting Attractors and Its Adaptive Synchronization

Rameshbabu Ramar*[1] and Sundarapandian Vaidyanathan[2]

[1*] Department of Electronics and Communication Engineering , VSB Engineering College , Karur, Tamil Nadu, India - 639111
Email: rrameshbabu15@gmail.com, Mobile No. +91 8015166025
[2]Centre for Control Systems , Vel Tech University , 400 Feet Outer Ring Road, Vel Nagar, Avadi, Chennai-600062 , Tamil Nadu, India
Email: sundar@veltech.edu.in, Mobile No. +91 9566113754

October 1, 2023

Abstract

In this paper, a new chaotic system with three sinusoidal nonlinearities is reported. The basic behavior of the new chaotic system is analyzed by means of equilibrium points, stability, and Lyapunov exponents. The new system has countably infinite number of equilibrium points, which is a novel feature of the system. The new system has multiple interesting features such as topologically different attractors, coexisting attractors, offset-boosted attractors, and polarity reversed offset-boosting attractors. These special features are analyzed and verified using classical tools such as bifurcation diagrams, Lyapunov exponent plots, and attractor diagrams. The bifurcation analysis and simulation results show that the proposed system has rich chaotic dynamics. Furthermore, the adaptive synchronization of the new system is achieved using a nonlinear feedback control methodology. MATLAB plots are shown to illustrate the control results for the new chaotic system with three sinusoidal nonlinearities.

Keywords: Chaotic system, Dynamic analysis, Coexisting attractors, Offset boosting, Adaptive synchronization.

1 Introduction

The chaos theory deals with the dynamical behavior of nonlinear dynamical systems which are highly sensitive to initial conditions and system parameters. Chaos has many applications in the field of science and engineering such as

navigation of mobile robots [1,2], analog to digital converters [3] medical image processing [4,5], investigation of HIV virus [6] and Internet of Things [7–9].

Many chaotic systems are introduced with unique features such as self-excited attractors [10,11], hidden attractors [12,13], coexisting attractors [14,15], infinitely many shifted attractors [16,17], multi scroll attractors [18,19], memristor attractors [20,21] and fractional order [22].

The chaotic attractors can be classified as self-excited attractors and hidden attractors. The self-excited attractors [23–25] can be detected using the unstable equilibrium points while the hidden attractors can be observed in the no equilibrium system [26–28]. Many systems have been designed with no equilibrium [29,30], stable equilibrium [31–33], line and curve of equilibrium [34–36], non-hyperbolic equilibrium [37–39] and infinitely many equilibria [40,41]. The chaotic system with amplitude control and offset boosting control are reported in many papers [42–45].

It has been of great interest to design a new offset boostable chaotic system with topologically different and multistability attractors. The multiple coexisting attractors can be realized in a chaotic system with fixed parameter values and different initial conditions. In [46], six different self-excited chaotic attractors are generated for different values of system parameters and realized initial condition based on multiple coexisting attractors. In [47], three different attractors are generated based on the equilibrium and initial conditions. This initial condition-based multiple attractor behavior is realized in many chaotic systems such as Gyrostat system [48], memristive system [49], unified system [50], conservative system [51], neuron system [52] and chemical oscillator [53] etc.

Infinitely many shifted attractors or offset-boosted attractors can also be realized in a particular chaotic system with fixed initial conditions and different parameter values. The dc offset boosting means that the attractor of the particular system can be shifted in any dimension in phase space. It is easy and convenient to switch the chaotic signal from bipolar to unipolar for various engineering applications such as Analog to Digital circuit chips, digital information transmission and signal conditioning circuits. The offset-boosted chaotic system can also be used to reduce the modulation devices in digital information systems. In 2016, Li and Sprott [54] realized the dc offset boosting in a chaotic system by introducing a single constant value. In the recent years, the offset boosting of chaotic signals has become an active area of research in chaotic literature and many scholars have applied the method to their proposed chaotic systems. In some of the systems [55–59], both initial conditions triggered coexisting attractors and offset boosting coexisting attractors have been realized.

One of the main practical applications of chaotic systems is secure communication in which the chaotic systems can act as the transmitter (master system) and receiver (slave system). In the past few decades, chaos synchronization has received great attention owing to its applications in designing secure communication systems. Various adaptive synchronization schemes have been developed in recent years such as sliding mode controller [60, 61], backstepping neural network method [62,63], observer-based synchronization [64] and so on.

In this research paper, a new offset boostable chaotic system with three sinusoidal nonlinearities is presented and the adaptive synchronization of the proposed system for the application of secure communication is also discussed. The proposed system has the following novel features:

- The system has countably infinite number of equilibrium points.
- The system generates topologically different attractors, one-wing, two wing and seven-scroll attractors.
- The system generates initial condition-oriented multiple coexisting attractors.
- The system generates offset boosting oriented infinitely many coexisting attractors.
- The system generates polarity reversed coexisting multiple attractors.

The remaining sections of this paper are organized as follows. In Section 2, the mathematical model of a new dc offset boostable chaotic system is introduced and its basic properties are analyzed. In Section 3, the topologically different attractors of the proposed system are verified using bifurcation diagrams. In section 4, the multistability and coexisting attractors of the proposed chaotic system are analyzed using bifurcation diagram and phase plots. In Section 5, the offset boosting oriented infinitely many coexisting attractors and polarity control behavior of the proposed chaotic system are discussed with Lyapunov exponent diagrams and phase plots. In Section 6, the adaptive synchronization of the proposed system is addressed for the practical applications. Finally, the conclusions are summarized in Section 7.

2 Design and Analysis of New Chaotic System

Lai *et al.* [65] introduced a new chaotic system as given in (1).

$$\begin{aligned} \dot{x} &= ax - yz \\ \dot{y} &= -by + xz \\ \dot{z} &= -cz + xyz + k \end{aligned} \tag{1}$$

In the Lai system (1), x,y and z are the state variables and a,b,c,k are the parameters of system (1). It was shown in [65] that the Lai system is chaotic for (a, b, c, k)=$(4, 9, 4, 4)$. The Lyapunov exponents of Lai system (1) are found as $l_1 = 1.7729$, $l_2 = 0$ and $l_3 = -7.5949$. Also, the Lyapunov dimension of the Lai system (1) is found as $D_L = 2.2334$. The Lai system (1) presents one scroll and initial condition-oriented coexisting attractors. We are motivated by the Lai system [65] to design a new chaotic system with topologically different strange attractors, one-wing attractors, two-wing attractors, seven scroll attractors, multi-stability and coexisting attractors, offset boosting attractors and

phase reversal attractors. The distance between the initial condition-oriented coexisting attractors can also be controlled in the new chaotic system.

The new chaotic system (2) is designed by introducing a sinusoidal nonlinearity in the first differential equation, two sinusoidal nonlinearities in the second differential equation and replacing the term xyz by cxy in the third differential equation of (1). Thus, the mathematical model of new chaotic system is in the form of Eq. (2).

$$\begin{aligned} \dot{x} &= a\sin x - cyz \\ \dot{y} &= b\sin x + z\sin x \\ \dot{z} &= c(xy - z) + d \end{aligned} \tag{2}$$

Here x,y and z are the signal variables of new system (2), a,b,c and d are the system bifurcation parameters. The proposed system (2) has some interesting multiple features for various system parameter values such as topologically different attractors, coexisting attractors, dc offset boosting and multi-scroll attractors. The parameter values c and d are chosen as 4 and 36.5 respectively and other parameter values are mentioned in Table. 1. Figure 1 and Figure 2 show the attractors of new system (2) in yz and xy plane respectively.

In this work, Wolf algorithm is used to calculate the Lyapunov exponents of the system (2) with the initial condition $(-1, 0, 1)$ and simulation time $t = 1E4$ sec. Then, Lyapunov dimension (D_L) of the system (2) is calculated using the Eq. (3).

$$D_L = 2 + \frac{l_1 + l_2}{|l_3|} \tag{3}$$

Table. 2 shows the Lyapunov exponent values (l_1, l_2, l_3) and their corresponding Lyapunov dimension value (D_L) for all cases. Table. 2 indicates that the proposed system (2) has fractal chaotic behaviour within itself. It also indicates that the system (2) has highly complex behavior in cases 4 and 5. The divergence l_T of the system (2) is calculated by adding all the Lyapunov exponent values $(l_T = l_1 + l_2 + l_3)$. The negative values obtained for l_T indicate that the system (2) is dissipative for all cases.

The equilibrium points for the proposed system can be obtained by equating $\dot{x} = 0$,$\dot{y} = 0$ and $\dot{z} = 0$ in (2) as given in Eq. (4).

$$a\sin x - cyz = 0 \tag{4a}$$

$$(b + z)\sin x = 0 \tag{4b}$$

$$c(xy - z) + d = 0 \tag{4c}$$

From Eq. (4b), we have two cases to consider: (A) $\sin x = 0$ and (B) $\sin x \neq 0$.

First, we consider the Case (A), when $\sin x = 0$. In this case, Eq. (4a) reduces to $yz = 0$. Either $y = 0$ or $z = 0$. When $y = 0$, Eq. (4c) gives $cz = d$ or $z = \frac{d}{c}$.

In this case, we have a countably infinity number of equilibrium points given by

$$E_n = \left(n\pi, 0, \frac{d}{c}\right), \quad (n \text{ is any integer}) \tag{5}$$

Next, we consider the case when $\sin x = 0$ and $z = 0$. In this case, Eq. (4c) gives $cxy + d = 0$. When $x = 0$, the equation $cxy + d = 0$ has no solution. When $x = n\pi$, where n is a non-zero integer, we get $y = -\frac{d}{cn\pi}$. Thus, we have a countably infinite number of equilibrium points given by

$$F_n = \left(n\pi, -\frac{d}{cn\pi}, 0\right), \quad (n \text{ is any non-zero integer}) \tag{6}$$

Next, we consider the case (B), when $\sin x \neq 0$. In this case, Eq. (4b) yields $b + z = 0$ or $z = -b$. Then the equilibrium points are obtained by solving the following system:

$$\begin{aligned} a\sin x + bcy &= 0 \\ c(xy + b) + d &= 0 \end{aligned} \tag{7}$$

For specific values of a, b, c, d, the two algebraic equations (7) can be solved to obtain the values of x and y.

To discuss the stability type of the equilibrium points of the proposed system (2), we suppose that the parameters a, b, c, d are positive constants. We calculate the Jacobian matrix and obtain the following:

$$J = \begin{vmatrix} a\cos x & -cz & -cy \\ (b+z)\cos x & 0 & \sin x \\ cy & cx & -c \end{vmatrix} \tag{8}$$

If we choose $\sin x = 0$, then the system (2) has countably infinite equilibrium points given by E_n (where n is an integer) and F_n (where n is a non-zero integer) as defined in the equations (5) and (6).

First, we discuss the stability type of the equilibrium points E_n, when n is an even integer. For this case, $\sin x = 0$ and $\cos x = 1$. Hence, the Jacobian matrix at E_n is given by

$$J = \begin{vmatrix} a & -d & 0 \\ b + \frac{d}{c} & 0 & 0 \\ 0 & cn\pi & -c \end{vmatrix} \tag{9}$$

which has the characteristic equation

$$(\lambda + c)[\lambda^2 - a\lambda + d(b + d/c)] = 0 \tag{10}$$

Hence, the Jacobian matrix J has the eigenvalue $\lambda = -c$ and the other two eigenvalues are roots of the characteristic equation

$$\lambda^2 - a\lambda + d(b + d/c) = 0 \tag{11}$$

By Routh-Hurwitz criterion, we know that the quadratic equation (11) has a positive real root and a negative real root. This shows that the equilibrium points E_n are saddle points and unstable, when n is an even integer.

Next, we discuss the stability type of the equilibrium points E_n, when n is an odd integer. For this case, $\sin x = 0$ and $\cos x = -1$. Hence, the Jacobian matrix at E_n is given by

$$J = \begin{vmatrix} -a & -d & 0 \\ -b - \frac{d}{c} & 0 & 0 \\ 0 & cn\pi & -c \end{vmatrix} \tag{12}$$

which has the characteristic equation

$$(\lambda + c)[\lambda^2 + a\lambda - d(b + d/c)] = 0 \tag{13}$$

Hence, the Jacobian matrix J has the eigenvalue $\lambda = -c$ and the other two eigenvalues are roots of the characteristic equation

$$\lambda^2 + a\lambda - d(b + d/c) = 0 \tag{14}$$

By Routh-Hurwitz criterion, we know that the quadratic equation (14) has a positive real root and a negative real root. This shows that the equilibrium points E_n are saddle points and unstable, when n is an odd integer.

Combining the two cases, we conclude that the equilibrium points E_n are saddle points and unstable, where n is any integer.

Next, we discuss the stability type of the equilibrium points F_n where n is an even integer. In this case, $\sin x = 0$ and $\cos x = 1$.

Hence, the Jacobian matrix at F_n is given by

$$J = \begin{vmatrix} a & 0 & \frac{d}{n\pi} \\ b & 0 & 0 \\ -\frac{d}{n\pi} & cn\pi & -c \end{vmatrix} \tag{15}$$

which has the characteristic equation

$$\lambda^3 + (c - a)\lambda^2 + \lambda\left(\frac{d^2}{n^2\pi^2} - ac\right) - bcd = 0. \tag{16}$$

By Routh-Hurwitz stability criterion, the characteristic equation (16) has unstable roots.

Thus, we conclude that the equilibrium points F_n are unstable, when n is an even integer.

In a similar manner, we can use Routh-Hurwitz stability criterion to establish that the equilibrium points F_n are unstable, when n is an odd integer. Combining the two cases, we conclude that the equilibrium points F_n are unstable, where n is any integer.

If we choose $\sin x \neq 0$, then $z = -b$ for an equilibrium point and the values of x and y of the equilibrium point can be obtained by solving the system (7) as given in Table. 3 which indicates that all the equilibrium points of system (2) are unstable saddle points.

3 Evolution of Topologically Different Attractors

The proposed system (2) presents six different types of attractors for various values of system parameters as given in Table. 1. In this section, this special behavior of the proposed system (2) is analyzed and verified by plotting the bifurcation diagram and Lyapunov exponent spectrum under the parameter a.The bifurcation diagram and Lyapunov plots can be plotted by varying the system parameter a and keeping others as constant. In this paper, the variation of λ_1, λ_2 and λ_3 are represented in blue, red and green colors respectively in all the Lyapunov exponent plots.

3.1 Under the parameters $a \in [1, 2]$, $(b, c, d) = (1, 4, 36.5)$

The bifurcation diagram and Lyapunov exponents spectrum under the parameters $a \in [1, 2]$ and (b, c, d)=$(1, 4, 36.5)$ with the initial condition $(-1, 0, 1)$ is shown in Figure 3. It is observed from the Figure 3a that the system (2) has broken bifurcation diagram and the system (2) has two wing chaotic attractor in the region $a \in [1, 1.13]$, one wing chaotic attractor in the region $a \in [1.25, 1.6]$. It is also observed from Figure 3a that there is a change in the amplitude level in the region $a \in [1.25, 1.35]$, $a \in [1.36, 1.57]$ and $a \in [1.58, 1.6]$ and thus the system (2) presents different chaotic attractors in this regions. Figure 3b shows the corresponding Lyapunov exponent plot and indicates that the system presents periodic attractor beyond $a = 1.6$. Figures (3c-3e) represent the various chaotic and periodic attractors in the region $a \in [1, 2]$ and (b, c, d)=$(1, 4, 36.5)$.

3.2 Under the parameters $a \in [1, 3]$, (b, c, d)=$(10, 4, 36.5)$

The bifurcation diagram under the parameters $a \in [1, 3]$ and $(b, c, d) = (10, 4, 36.5)$ with the initial condition $(-1, 0, 1)$ is shown in Figure 4a which indicates that the system (2) produces seven-scroll attractor in the region $a \in [1, 2.25]$ and single scroll attractor in the region $a \in [2.3, 2.55]$. Since there is a change in the amplitude level beyond $a = 2.55$, system (2) presents different attractors in this region. Figure 4b represents the corresponding Lyapunov exponent plot under the parameter a. Figure 4c represents the seven-scroll chaotic attractor at $a = 1.5$ in the (x, y) plane. Figure 4d represents one scroll attractor at $a = 2.5$ (Blue) and $a = 2.6$ (Red) in (x, y) plane.

4 Evolution of Multistability and Coexisting Attractors

Multistability for a chaotic system means that the chaotic system under consideration produces multiple attractors for the same set of parameter values but different initial conditions. The proposed system (2) presents multiple coexisting attractors for case 2 and case 5 mentioned in Table 1 for various initial

conditions. This special behavior can be verified using bifurcation diagram and attractor diagram as given in Figures 5 - 7. In order to demonstrate the coexisting attractor behavior, the bifurcation diagram of system (2) is plotted with the initial conditions $X_1 = (-1, 0, 1)$ (Blue) and $X_2 = (1, 0, -1)$ (Red).

4.1 Under the parameters $a \in [1, 2]$, $(b, c, d) = (1, 4, 36.5)$

Figure 5a shows the bifurcation diagram under the parameter a in the region $a\epsilon[1 - 2]$, $(b, c, d) = (1, 4, 36.5)$ with the initial conditions X_1 (Blue) and X_2 (Red). It is observed in Figure 5a that there is no overlapping of bifurcation amplitude $xmax$ in the small regions $a \in [1.14, 1.17]$, $a \in [1.25, 1.31]$, $a \in [1.4, 1.47]$ and $a \in [1.59, 1.69]$. Thus, the new system (2) produces coexisting multiple chaotic and periodic attractors in these particular regions. Figures (5b - 5d) represent the various coexisting chaotic and periodic attractor diagrams in the region $a\epsilon[1 - 2]$.

4.2 Under the parameters $b \in [0.75, 1.1]$, $(a, c, d) = (1.3, 4, 36.5)$

Figure 6a shows the bifurcation diagram under the parameter b in the region $b \in [0.75, 1.1]$ and $(a, c, d) = (1.3, 4, 36.5)$ with the initial conditions X_1 (Blue) and X_2 (Red). It can be observed from Figure 6a and the Lyapunov exponent diagram given in Figure 6b that there is no overlapping of amplitude in the region $b \in [0.75, 1.05]$. It is also noted that the chaotic and periodic states are still unchanged for the different initial conditions. The system (2) has forward bifurcation phenomena under this parameter which means that the periodic attractors are detected in the region $b \in [0.75, 0.96]$ and chaotic attractors are detected beyond $b = 0.96$. Figures (6c - 6f) show the various coexisting periodic and chaotic attractors in the region $b \in [0.75, 1.1]$.

4.3 Under the parameters $d \in [36, 38.5]$, (a, b, c)=$(1.3, 1, 4)$

Figure. 7a shows the bifurcation diagram under the parameter d in the region $d \in [36 - 38.5]$ and (a, b, c)=$(1.3, 1, 4)$ with the initial conditions X_1 (Blue) and X_2 (Red).It can be observed from Figure 7a that there is no overlapping of amplitude in the region $d \in [36.4, 38.5]$ and the chaotic and periodic states are unchanged under the parameter d also.The system (2) has chaotic attractors in the region $d \in [36, 37.3]$ and then periodic attractors in the region $d \in [37.3, 38.5]$. It is evident that the system experiences reverse bifurcation under the parameter d.

5 Evolution of Offset Boosting

One of the main issues in the chaos control is offset boosting which means the change of position of the attractor in phase space. This can be realized in a particular chaotic system by introducing an offset booster with any one of its

state variables. The introduction of booster value increases or decreases the average value of that particular signal and changes its location. If the signal appears in multiple times in the system, this particular behavior can be realized by adding multiple booster values with the signal. Recently, Chunbiao Li [66] demonstrated parameter-oriented, initial condition-oriented offset boosting and polarity control behavior in VB14 based chaotic systems. The author realized the various offset boosting attractors in VB14 system by introducing a constant parameter, periodic function and trigonometric functions.

In the proposed system (2), offset boosting control along the y dimension can be realized for various booster value δ when $a = (1.5, 2.5, 2.6)$, $b = 10$, $c = 4$ and $d = 36.5$. The new chaotic system with booster parameter is given in Eq. (17).

$$\begin{aligned} \dot{x} &= a\sin x - c(y+\delta)z \\ \dot{y} &= b\sin x + z\sin x \\ \dot{z} &= c[x(y+\delta) - z] + d \end{aligned} \tag{17}$$

5.1 Offset boosting for the parameters (a, b, c, d)=$(1.5, 10, 4, 36.5)$

The system (17) presents infinitely many shifted attractors along y direction when $a = 1.5$ for various values of δ. This is shown in Figure 8 in which $\delta = 0$ (Blue), $\delta = 8$ (Red), $\delta = -8$ (Green). Figures 8a-8b show the coexisting offset boosted attractors in (x, y) and (y, z) planes. Figure 8c represents the time variation of the offset boosted signal y. Figure 8d shows the Lyapunov exponent plot of (2) under $\delta \in [-8, 8]$. It can be concluded from Figure 8d that the booster value does not affect the Lyapunov exponent values of the new system (2).

5.2 Offset boosting with multistability for the parameters (a, b, c, d)=$(2.5, 10, 4, 36.5)$

The system (2) also presents both initial condition-oriented coexisting attractors and offset boosting oriented coexisting attractors simultaneously when $a = 2.5$. This is shown in Figures 9a and 9b in which blue and red colors represent the coexisting attractors with $\delta = 0$ under $(-1, 0, 1)$ (Blue) and $(1, 0, -1)$ (Red), green and cyan colors represent the coexisting attractors with $\delta = 1$ under $(-1, 0, 1)$ (Green) and $(1, 0, -1)$ (Cyan), magenta and yellow colors represent the coexisting attractors with $\delta = -1$ under $(-1, 0, 1)$ (Magenta) and $(1, 0, -1)$ (Yellow). It can be concluded that the distance between the coexisting attractors can be controlled in the proposed system (2).Figure 9c represents the offset boosted attractors in yz plane with $\delta = 0$ (Blue), $\delta = 2$ (Red) and $\delta = -2$ (Green) with initial condition $(-1, 0, 1)$ for all attractors. Figure 9d shows that the offset booster does not change the chaotic behavior of the system in the region $\delta \in [-1, 1]$.

5.3 Offset boosting with polarity reversal for the parameters (a, b, c, d)=$(2.6, 10, 4, 36.5)$

The offset boosting in the system (2) introduces polarity reversal for negative values of δ when $a = 2.6$. Even though the offset boosting in the y dimension does not change the polarity of the left-hand side of system (18) for a negative value of δ, it introduces polarity reversal. Figure 10 represents the polarity reversal in which $\delta = 6$ (Blue), $\delta = 10$ (Green), $\delta = 14$ (Magenta), $\delta = -6$ (Red), $\delta = -10$ (Cyan), $\delta = -14$ (Yellow) and the initial condition $(-1, 0, 1)$ is chosen for all the attractors. Figure 10c indicates that the Lyapunov spectrum of system (17) is not modified by an offset booster in the region $\delta \in [-10, 10]$.

$$\begin{aligned} \dot{x} &= a \sin x - c(y - \delta)z \\ \dot{y} &= b \sin x + z \sin x \\ \dot{z} &= c[x(y - \delta) - z] + d \end{aligned} \tag{18}$$

6 Adaptive Synchronization of the New Chaotic System

In this section, the adaptive synchronization of identical new chaotic system is achieved by using master-slave adaptive feedback control method. The synchronization result is verified using the Lyapunov stability theory.

The master system and slave system are given in Eq. (19) and Eq. (20) respectively as follows:

$$\begin{aligned} \dot{x_1} &= a \sin x_1 - c y_1 z_1 \\ \dot{y_1} &= b \ sin x_1 + z_1 \sin x_1 \\ \dot{z_1} &= c(x_1 y_1 - z_1) + d \end{aligned} \tag{19}$$

$$\begin{aligned} \dot{x_2} &= a \sin x_2 - c y_2 z_2 + U_1 \\ \dot{y_2} &= b \sin x_2 + z_2 \sin x_2 + U_2 \\ \dot{z_2} &= c(x_2 y_2 - z_2) + d + U_3 \end{aligned} \tag{20}$$

The synchronization errors can be defined as $e_1 = x_2 - x_1$, $e_2 = y_2 - y_1$,$e_3 = z_2 - z_1$ and the error dynamics can be obtained from Eq. (19) and Eq. (20) as given in Eq. (21).

$$\begin{aligned} \dot{e}_1 &= a[\sin x_2 - \sin x_1] + c(y_1 z_1 - y_2 z_2) + U_1 \\ \dot{e}_2 &= b[\sin x_2 - \sin x_1] + z_2 \sin x_2 - z_1 \sin x_1 + U_2 \\ \dot{e}_3 &= c[x_2 y_2 - x_1 y_1 - e_3] + U_3 \end{aligned} \tag{21}$$

Now, the adaptive controllers [U_1,U_2,U_3] for the synchronization of the pro-

posed system can be obtained as Eq. (22) with the following equations:

$$\begin{aligned} U_1 &= -\hat{a}[\sin x_2 - \sin x_1] - \hat{c}[y_1 z_1 - y_2 z_2] - G_1 e_1 \\ U_2 &= -\hat{b}[\sin x_2 - \sin x_1] - z_2 \sin x_2 + z_1 \sin x_1 - G_2 e_2 \\ U_3 &= -\hat{c}[x_2 y_2 - x_1 y_1 - e_3] - G_3 e_3 \end{aligned} \tag{22}$$

Here, G_1,G_2 and G_3 are the positive gains and $\hat{a}$,$\hat{b}$ and $\hat{c}$ are the estimates of unknown parameters a,b and c respectively. By substituting the Eq. (22) in Eq. (21), we get the following closed-loop error dynamics:

$$\begin{aligned} \dot{e}_1 &= e_a[\sin x_2 - \sin x_1] + e_c[y_1 z_1 - y_2 z_2] - G_1 e_1 \\ \dot{e}_2 &= e_b[\sin x_2 - \sin x_1] - G_2 e_2 \\ \dot{e}_3 &= e_c[x_2 y_2 - x_1 y_1 - e_3] - G_3 e_3 \end{aligned} \tag{23}$$

Here, $e_a = a - \hat{a}$, $e_b = b - \hat{b}$, $e_c = c - \hat{c}$ and thus $\dot{e_a} = -\dot{\hat{a}}$, $\dot{e_b} = -\dot{\hat{b}}$, $\dot{e_c} = -\dot{\hat{c}}$. Now, consider the Lyapunov stability function as given in Eq. (24),

$$\dot{V} = e_1 \dot{e}_1 + e_2 \dot{e}_2 + e_3 \dot{e}_3 + e_a \dot{e}_a + e_b \dot{e}_b + e_c \dot{e}_c \tag{24}$$

By substituting Eq. (23) in Eq. (24), we obtained that

$$\begin{aligned} \dot{V} = -[G_1 e_1^2 + G_2 e_2^2 + G_3 e_3^2] + e_a[e_1(sinx_2 - sinx_1) - \dot{\hat{a}}] + e_b[e_2(sinx_2 - sinx_1) - \dot{\hat{b}}] \\ + e_c[e_1(y_1 z_1 - y_2 z_2 + e_3(x_2 y_2 - x_1 y_1 - e_3) - \dot{\hat{c}}] \end{aligned} \tag{25}$$

In view of Eq. (25), the parameter update law can be chosen as,

$$\begin{aligned} \dot{\hat{a}} &= e_1(\sin x_2 - \sin x_1) \\ \dot{\hat{b}} &= e_2(\sin x_2 - \sin x_1) \\ \dot{\hat{c}} &= e_1[y_1 z_1 - y_2 z_2 + e_3(x_2 y_2 - x_1 y_1 - e_3)] \end{aligned} \tag{26}$$

From the equations (25) and (26), the time derivative of the Lyapunov function can be obtained as,

$$\dot{V} = -G_1 e_1^2 - G_2 e_2^2 - G_3 e_3^2 \tag{27}$$

which is a negative semi-definite function.

Using Barbalat's lemma and Lyapunov stability theory, we conclude that the closed-loop system (23) is globally asymptotically stable for all initial values of the error signals e_1, e_2, e_3 by using the adaptive controller (22) and adaptive parameter law (26).

The mathematical results for adaptive synchronization derived in this section is verified with the following conditions

- The system parameters are chosen as $a = 1.3$, $b = 1$, $c = 4$,$d = 36.5$.

- The initial conditions for master and slave system are chosen as (-1,0,1) and (1,0,-1) respectively.
- The initial conditions for parameters are chosen as $a(0) = 1$,$b(0) = -1$ and $c(0) = 1$.
- The gains are chosen as $G_1 = G_2 = G_3 = 1$.

Figure 11 represents the unsynchronized and synchronized state variables with initial conditions (-1,0,1) (blue) and (1,0,-1) (red).

7 Conclusion

In this paper, a chaotic system with three sinusoidal nonlinearities is introduced and analysed its special behaviors such as countably infinite number of equilibrium points, different attractors, coexisting attractors and offset-boosting attractors. The proposed system exhibits different six types of attractors which are verified using bifurcation diagrams and Lyapunov exponent plots. The attractors of the proposed system can be offset-boosted for the particular parameter values. The coexisting attractors and offset-boosted attractors are verified and analyzed in detail with the help of bifurcation diagram and Lyapunov exponent plots. The Lyapunov exponent plots under offset booster parameter have constant values which indicates that the booster parameter does not modify the stability and chaotic behavior of the proposed system. Finally, the proposed system is adaptively synchronized for the application of secure communication systems. The mathematical and simulation results indicate that the proposed system has very wealthy chaotic dynamics and can be used for secure communication systems.

References

[1] Nwachioma, C. and Pérez-Cruz, J.H. "Analysis of a new chaotic system, electronic realization and use in navigation of differential drive mobile robot", *Chaos, Solitons & Fractals*, **144**, Article ID 110684 (2021).

[2] Wu, L., Wang, D., Zhang, C., et al. "Chaotic synchronization in mobile robots", *Mathematics*, **10** (23), Article ID 4568 (2022).

[3] Shen, Y., Bai, Y., Zou, T., et al. "Dynamical analysis of a new chaotic system and its application in ADC", *Physica Scripta*, **97** (8), Article ID 085202 (2022).

[4] Li, M., Pan, S., Meng, W., et al. "Medical image encryption algorithm based on hyper-chaotic system and DNA coding", *Cognitive Computation and Systems*, **4**(4), pp. 378–390 (2022).

[5] Liu, J., Ma, Y., Li, S., et al. "A new simple chaotic system and its application in medical image encryption", *Multimedia Tools and Applications*, **77**, pp. 22787–22808 (2018).

[6] Parastesh, F., Aram, Z., Namazi, H., et al. "A simple chaotic model for development of HIV virus", *Scientia Iranica*, **28**(3), pp. 1643-1652 (2021).

[7] Durga, R., Poovammal, E., Ramana, K., et al. "CES blocks—a novel chaotic encryption schemes-based blockchain system for an IoT environment", *IEEE Access*, **10**, pp. 11354-11371 (2022).

[8] Meshram, C., Ibrahim, R.W., Obaid, A.J., et al. "Fractional chaotic maps based short signature scheme under human-centered IoT environments", *Journal of Advanced Research*, **32**, pp. 139-148 (2021).

[9] Li, L., El-Latif, A., Ahmed, A., et al. "Multimedia cryptosystem for IoT applications based on a novel chaotic system around a predefined manifold", *Sensors*, **22**(1), Article ID 334 (2022).

[10] Xu, G., Shekofteh, Y., Akgül, A., et al. "A new chaotic system with a self-excited attractor: Entropy measurement, signal encryption, and parameter estimation", *Entropy*, **20**(2), Article ID 86 (2018).

[11] Faghani, Z., Nazarimehr, F., Jafari, S., et al. "Simple chaotic systems with specific analytical solutions", *International Journal of Bifurcation and Chaos*, **29**(09), Article ID 1950116 (2019).

[12] Pham, V.T., Volos, C., Jafari, S., et al. "A chaotic system with different families of hidden attractors", *International Journal of Bifurcation and Chaos*, **26**(08), Article ID 1650139 (2016).

[13] Ouannas, A., Khennaoui, A.A., Momani, S., et al. "Hidden attractors in a new fractional–order discrete system: Chaos, complexity, entropy, and control", *Chinese Physics B*, **29**(5), Article ID 050504 (2020).

[14] Lai, Q., Wan, Z., Kuate, P.D.K., et al. "Coexisting attractors, circuit implementation and synchronization control of a new chaotic system evolved from the simplest memristor chaotic circuit", *Communications in Nonlinear Science and Numerical Simulation*, **89**, Article ID 105341 (2020).

[15] Lai, Q., Wan, Z. and Kamdem Kuate, P.D. "Modelling and circuit realisation of a new no-equilibrium chaotic system with hidden attractor and coexisting attractors", *Electronics Letters*, **56**(20), pp. 1044-1046 (2020).

[16] Lai, Q., Kuate, P.D.K, Pei, H., et al. "Infinitely many coexisting attractors in no-equilibrium chaotic system", *Complexity*, **2020**, Article ID 8175639 (2020).

[17] Wen, J. and Wang, J. "A chaotic system with infinite attractors based on memristor", *Frontiers in Physics*, **10**, Article ID 375 (2022).

[18] Sugandha, K. and Singh, P.P. "Generation of a multi-scroll chaotic system via smooth state transformation", *Journal of Computational Electronics*, **21**(4), pp. 781–791 (2022).

[19] Liu, S., Wei, Y., Liu, J., et al. "Multi-scroll chaotic system model and its cryptographic application", *International Journal of Bifurcation and Chaos*, **30**(13), Article ID 2050186 (2020).

[20] Yan, D., Wang, L., Duan, S., et al. "Chaotic attractors generated by a memristor-based chaotic system and Julia fractal", *Chaos, Solitons & Fractals*, **146**, Article ID 110773 (2021).

[21] Sun, J., Zhao, X., Fang, J., et al. "Autonomous memristor chaotic systems of infinite chaotic attractors and circuitry realization", *Nonlinear Dynamics*, **94**, pp. 2879–2887 (2018).

[22] Lassoued, A., Nazarimehr, F. and Boubaker, O. "Dynamics and circuit simulation of a fractional-order hyperchaotic system", *Scientia Iranica*, **30**(2), pp. 507–517 (2023).

[23] Zhang, S., Peng, J., Jin, S., et al. "Analysis of a new 3-D chaotic system with a self-excited attractor", *In 2020 IEEE 19th International Conference on Cognitive Informatics & Cognitive Computing*, Beijing, China, pp. 45–51 (2020).

[24] Sambas, A., Vaidyanathan, S., Zhang, S., et al. "A new 4-D chaotic system with self-excited two-wing attractor, its dynamical analysis and circuit realization", *In Journal of Physics: Conference Series*, **1179**(1), Article ID 012084 (2019).

[25] Sprott, J.C. "Some simple chaotic flows", *Physical Review E*, **50** (2), pp. 647–650 (1994).

[26] Zhang, S., Wang, X. and Zeng, Z. "A simple no-equilibrium chaotic system with only one signum function for generating multidirectional variable hidden attractors and its hardware implementation", *Chaos: An Interdisciplinary Journal of Nonlinear Science*, **30** (5), Article ID 053129 (2020).

[27] Lai, Q., Wan, Z. and Kuate, P.D.K. "Modelling and circuit realisation of a new no-equilibrium chaotic system with hidden attractor and coexisting attractors", *Electronics Letters*, **56** (20), pp. 1044–1046 (2020).

[28] Chowdhury, N.S. and Ghosh, D. "Hidden attractors: A new chaotic system without equilibria", *The European Physical Journal Special Topics*, **229**, pp. 1299–1308 (2020).

[29] Rameshbabu, R., Kavitha, K., Gomathi, P.S., et al. "A new hidden attractor hyperchaotic system and its circuit implementation, adaptive synchronization and FPGA implementation", *Nonlinear Dynamics & System Theory*, **23**(2), pp. 214–226 (2023).

[30] Wang, M. and Ma, S. "Hamilton energy control for the chaotic system with hidden attractors", *Complexity*, **2021**, Article ID 5530557 (2021).

[31] Vijayakumar, M.D., Karthikeyan, A., Zivcak, J., et al. "Dynamical behavior of a new chaotic system with one stable equilibrium", *Mathematics*,**9**(24), pp. 2227–7390 (2021).

[32] Wang, X., Akgul, A., Cicek, S., et al. "A chaotic system with two stable equilibrium points: Dynamics, circuit realization and communication application", *International Journal of Bifurcation and Chaos*, **27**(08), Article ID 1750130 (2017).

[33] Kapitaniak, T., Mohammadi, S.A., Mekhilef, S., et al. "A new chaotic system with stable equilibrium: Entropy analysis, parameter estimation, and circuit design", *Entropy*, **20**(9), Article ID 670 (2018).

[34] Nazarimehr, F. and Sprott, J.C. "Investigating chaotic attractor of the simplest chaotic system with a line of equilibria", *European Physical Journal: Special Topics*, **229**, pp. 1289–1297 (2020).

[35] Zhu, X. and Du, W.S. "New chaotic systems with two closed curve equilibrium passing the same point: Chaotic behavior, bifurcations, and synchronization", *Symmetry*, **11**(8), Article ID 951 (2019).

[36] Sambas, A., Vaidyanathan, S., Zhang, X., et al. "A novel 3D chaotic system with line equilibrium: multistability, integral sliding mode control, electronic circuit, FPGA implementation and its image encryption", *IEEE Access*, **10**, pp. 68057–68074 (2022).

[37] Li, C.L. and Xiong, J.B. "A simple chaotic system with non-hyperbolic equilibria", *Optik*, **128**, pp. 42–49 (2017).

[38] Rajagopal, K., Pham, V.T., Tahir, F.R., et al. "A chaotic jerk system with non-hyperbolic equilibrium: Dynamics, effect of time delay and circuit realisation", *Pramana*, **90**(52), pp. 1–8 (2018).

[39] Zolfaghari, N.M., Charmi, M. and Hassanpoor, H. "A new chaotic system with only nonhyperbolic equilibrium points: Dynamics and its engineering application", *Complexity*, **2022**, Article ID 4488971 (2022).

[40] Pham, V.T., Jafari, S. and Kapitaniak, T. "Constructing a chaotic system with an infinite number of equilibrium points", *International Journal of Bifurcation and Chaos*, **26**(13), Article ID 1650225 (2016).

[41] Kingni, S.T., Pham, V.T., Jafari, S., et al. "A chaotic system with an infinite number of equilibrium points located on a line and on a hyperbola and its fractional-order form", *Chaos, Solitons & Fractals*, **99**, pp.209-218 (2017).

[42] Mboupda Pone, J.R., Kingni, S.T., Kol, G.R., et al."Hopf bifurcation, antimonotonicity and amplitude controls in the chaotic Toda jerk oscillator: analysis, circuit realization and combination synchronization in its fractional-order form", *Automatika*, **60**(2), pp. 149–161 (2019).

[43] Wang, Z. and Liu, S. "Design and implementation of simplified symmetry chaotic circuit", *Symmetry*, **14**(11), Article ID 2299 (2022).

[44] Ma, C., Mou, J., Xiong, L., et al. "Dynamical analysis of a new chaotic system: asymmetric multistability, offset boosting control and circuit realization", *Nonlinear Dynamics*, **103**, pp. 2867–2880 (2021).

[45] Zhang, Z., Huang, L., Liu, J., et al. "A new method of constructing cyclic symmetric conservative chaotic systems and improved offset boosting control", *Chaos, Solitons & Fractals*, **158**, Article ID 112103 (2022).

[46] Rajagopal, K., Akgul, A., Moroz, I.M., et al. "A simple chaotic system with topologically different attractors", *IEEE Access*, **7**, pp. 89936–89947 (2019).

[47] Cao, H.Y. and Zhao, L. "A new chaotic system with different equilibria and attractors", *European Physical Journal Special Topics*, **230**, pp. 1905–1914 (2021).

[48] Marwan, M., Dos Santos, V., Abidin, M.Z., et al. "Coexisting attractor in a gyrostat chaotic system via basin of attraction and synchronization of two nonidentical mechanical systems", *Mathematics*, **10**(11), Article ID 1914 (2022).

[49] Zang, H., Gu, Z., Lei, T., et al. "Coexisting chaotic attractors in a memristive system and their amplitude control", *Pramana*, **94**(62) Article ID 62 (2020).

[50] Lai, Q. "A unified chaotic system with various coexisting attractors", *International Journal of Bifurcation and Chaos*, **31**(01), Article ID 2150013 (2021).

[51] Yan, M. and Xie, J. "A conservative chaotic system with coexisting chaotic-like attractors and its application in image encryption", *Journal of Control and Decision*, **10** (2), pp. 1–13 (2022).

[52] Bouallegue, K. "Gallery of chaotic attractors generated by fractal network", *International Journal of Bifurcation and Chaos*, **25**(01), Article ID 1530002 (2015).

[53] Kpomahou, Y.J.F., Adomou, A., Adéchinan, J.A., et al. "Chaotic Behaviors and Coexisting Attractors in a New Nonlinear Dissipative Parametric Chemical Oscillator", *Complexity*, **2022**, Article ID 9350516 (2022).

[54] Li, C. and Sprott, J.C. "Variable-boostable chaotic flows", *Optik*, **127**(22), pp. 10389–10398 (2016).

[55] Ramar, R. "Design of a New Chaotic System with Sine Function: Dynamic Analysis and Offset Boosting Control". *Chaos Theory and Applications*, **5**(2), pp. 118-126 (2023).

[56] Yan, S., Sun, X., Wang, Q., et al. "A novel double-wing chaotic system with infinite equilibria and coexisting rotating attractors: Application to weak signal detection", *Physica Scripta*, **96**(12), Article ID 125216 (2021).

[57] Wen, J., Feng, Y., Tao, X., et al. "Dynamical analysis of a new chaotic system: Hidden attractor, coexisting-attractors, offset boosting, and DSP realization", *IEEE Access*, **9**, pp. 167920–167927 (2021).

[58] Huang, L., Zhang, X., Zang, H., et al. "An Offset-Boostable Chaotic Oscillator with Broken Symmetry", *Symmetry*, **14**(9), Article ID 1903 (2022).

[59] Du, C., Liu, L., Lu, L., et al. "An offset boostable hidden circuit and its digital information transmission", *In 2022 IEEE 13th Annual Ubiquitous Computing, Electronics & Mobile Communication Conference (UEMCON)*, New York, USA, pp. 187–194 (2022).

[60] Vaidyanathan, S. "Sliding mode controller design for the global stabilization of chaotic systems and its application to Vaidyanathan jerk system", *Advances and Applications in Chaotic Systems*, pp. 537–552 (2016).

[61] Mostafaee, J., Mobayen, S., Vaseghi, B., et al. "Finite–time synchronization of a new five–dimensional hyper–chaotic system via terminal sliding mode control", *Scientia Iranica*, **30** (1), pp. 167–182 (2021).

[62] Sarbaz, M., Soltanian, M., Manthouri, M., et al. "Adaptive optimal control of chaotic system using backstepping neural network concept", *In 2022 8th International Conference on Control, Instrumentation and Automation (ICCIA)*, Tehran, Iran, pp. 1–5. IEEE (2022).

[63] Vaidyanathan, S., Pham, V.T. and Volos, C.K. "Adaptive backstepping control, synchronization and circuit simulation of a novel jerk chaotic system with a quartic nonlinearity", *Advances and Applications in Chaotic Systems*, pp. 109–135 (2016).

[64] Kabziński, J. and Mosiołek, P. "Adaptive, observer-based synchronization of different chaotic systems", *Applied Sciences*, **12** (7), Article ID 3394 (2022).

[65] Lai, Q., Akgul, A., Li, C., et al. "A new chaotic system with multiple attractors: Dynamic analysis, circuit realization and S-Box design", *Entropy*, **20** (1), Article ID 12 (2017).

[66] Chunbiao, L., Jiang, Y. and Xu, M.A. "On offset boosting in chaotic system", *Chaos Theory and Applications*, **3**(2), pp. 47–54 (2021).

Biographies

Rameshbabu Ramar received the P.HD degree in Electronics and Communication Engineering from St.Peter University at Chennai, Tamilnadu, India in 2021. He is currently a Associate Professor at the Department of Electronics and Communication Engineering, V.S.B Engineering College, Karur, Tamilnadu, India. He has published many Scopus-indexed research publications in international journals. His current research interests include chaotic and hyperchaotic systems, FPGA implementation, Adaptive control, and Chaos Synchronization.

Sundarapandian Vaidyanathan received the D.Sc. degree in Electrical and Systems Engineering from Washington University at St. Louis, St. Louis, MO, USA, in 1996. He is currently a Professor at the Research and Development Centre, Vel Tech University, Chennai, India. He has published over 600 Scopus-indexed research publications in international journals. His current research interests include linear and nonlinear control systems, chaotic and hyperchaotic systems, circuits, data science, mathematical modelling, and scientific computing.

List of Figure Caption

1. Figure 1: Attractors of the proposed system in yz plane when $c = 4$ and $d = 36.5$. (a) Two wing attractor, (b) One scroll attractor, (c) One scroll attractor, (d) Two wings attractor, (e) One wing attractor and (f) One wing attractor

2. Figure 2: Attractors of the proposed system in the xy plane for various values of a and b, while the parameters c and d are fixed at $c = 4$ and $d = 36.5$. (a) Two wings attractor, (b) One scroll attractor, (c) One scroll attractor, (d) Seven scroll attractor, (e) One wing attractor and (f) One wing attractor.

3. Figure 3: (a) Bifurcation diagram and (b) corresponding Lyapunov exponent plot for the parameter range $a \in [1, 2]$. (c) Two wing chaotic attractors when $a = 1.1$, (d) One wing attractors when $a = 1.3$ (Blue) and $a = 1.5$ (Red) and (e) Periodic attractor when $a = 1.65$. The remaining parameters are taken as $(b, c, d) = (1, 4, 36.5)$ and the initial conditions are chosen as $(-1, 0, 1)$.

4. Figure 4: (a) Bifurcation diagram and (b) the corresponding Lyapunov exponent plot under the parameter $a \in [1, 3]$. (c) Seven-scroll attractor in (x, y) plane when $a = 1.5$, (d) Single-scroll attractors in xy plane when $a = 2.5$ (Blue) and $a = 2.6$ (Red). The remaining parameters are taken as (b, c, d)=$(10, 4, 36.5)$.The initial conditions are chosen as $(-1, 0, 1)$.

5. Figure 5: (a) Bifurcation diagram for the region $a \in [1, 2]$,(b, c, d)=$(1, 4, 36.5)$ with the initial conditions X_1 (Blue) and X_2 (Red), (b) Coexisting chaotic

List of Tables

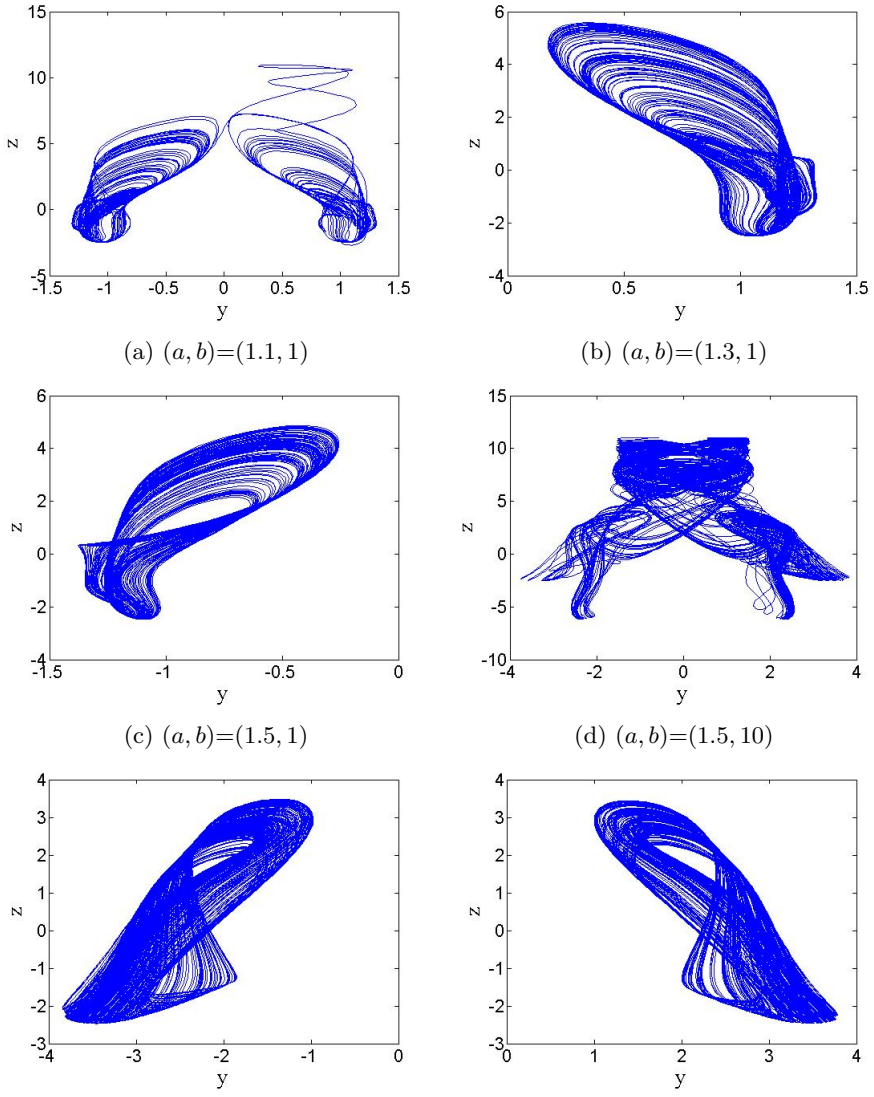

(a) (a, b)=(1.1, 1) (b) (a, b)=(1.3, 1)

(c) (a, b)=(1.5, 1) (d) (a, b)=(1.5, 10)

(e) (a, b)=(2.5, 10) (f) (a, b)=(2.6, 10)

Figure 1: Attractors of the proposed system in yz plane when $c = 4$ and $d = 36.5$. (a) Two wing attractor, (b) One scroll attractor, (c) One scroll attractor, (d) Two wings attractor, (e) One wing attractor and (f) One wing attractor.

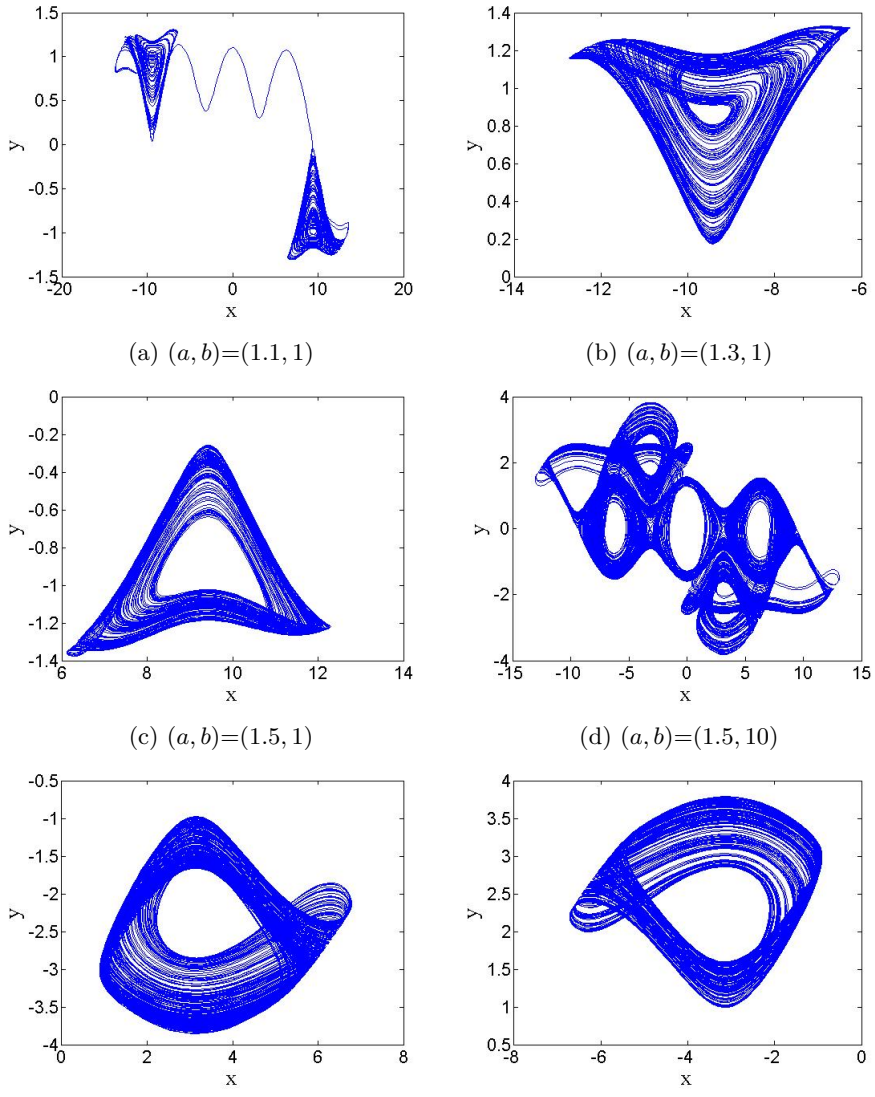

(a) (a, b)=$(1.1, 1)$ (b) (a, b)=$(1.3, 1)$

(c) (a, b)=$(1.5, 1)$ (d) (a, b)=$(1.5, 10)$

(e) (a, b)=$(2.5, 10)$ (f) (a, b)=$(2.6, 10)$

Figure 2: Attractors of proposed system in the xy plane for various values of a and b, while the parameters c and d are fixed at $c = 4$ and $d = 36.5$. (a) Two wings attractor, (b) One scroll attractor, (c) One scroll attractor, (d) Seven scroll attractor, (e) One wing attractor and (f) One wing attractor.

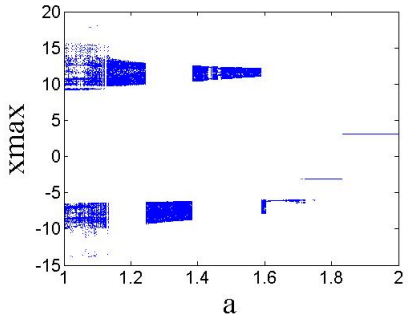

(a) Bifurcation diagram

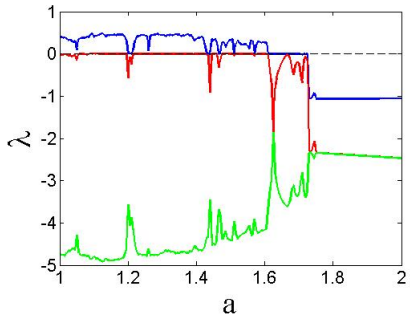

(b) Lyapunov exponent plot

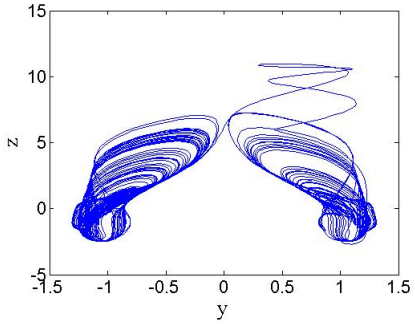

(c) $a = 1.1$

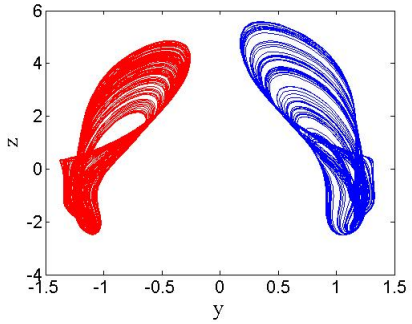

(d) $a = 1.3$ (Blue) and $a = 1.5$ (Red)

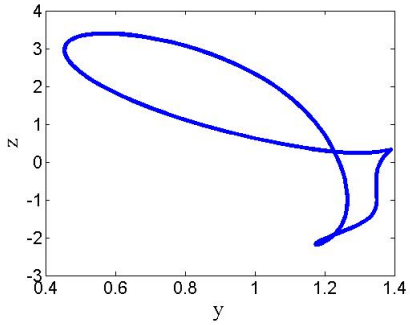

(e) Periodic attractor at $a = 1.65$

Figure 3: (a) Bifurcation diagram and (b) corresponding Lyapunov exponent plot for the parameter range $a \in [1, 2]$. (c) Two wing chaotic attractors when $a = 1.1$, (d) One wing attractors when $a = 1.3$ (Blue) and $a = 1.5$ (Red) and (e) Periodic attractor when $a = 1.65$. The remaining parameters are taken as $(b, c, d) = (1, 4, 36.5)$ and the initial conditions are chosen as $(-1, 0, 1)$.

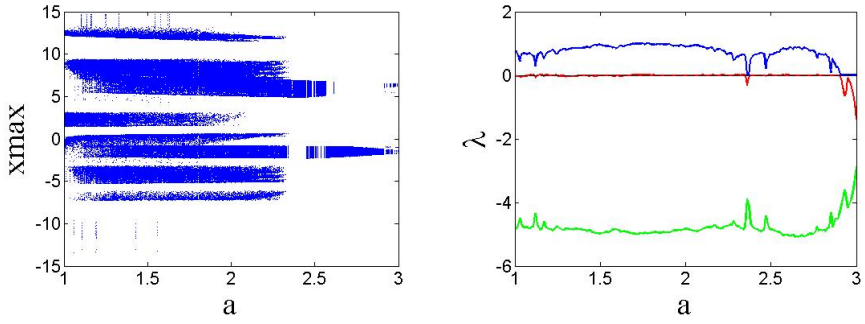

(a) Bifurcation diagram

(b) Lyapunov exponent plot

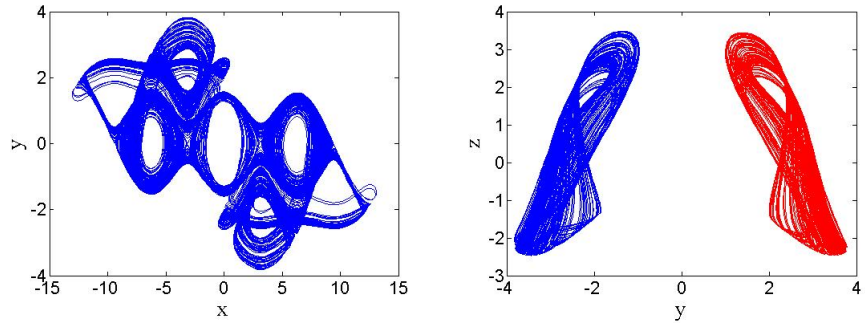

(c) $a = 1.5$

(d) $a = 2.5$(Blue) and $a = 2.6$(Red)

Figure 4: (a) Bifurcation diagram and (b) the corresponding Lyapunov exponent plot under the parameter $a \in [1, 3]$. (c) Seven-scroll attractor in (x, y) plane when $a = 1.5$, (d) Single-scroll attractors in xy plane when $a = 2.5$ (Blue) and $a = 2.6$ (Red). The remaining parameters are taken as (b, c, d)=$(10, 4, 36.5)$.The initial conditions are chosen as $(-1, 0, 1)$.

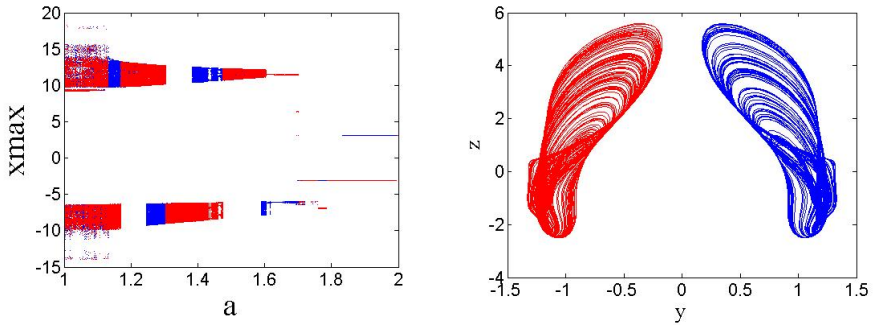

(a) Bifurcation diagram (b) $a = 1.3$

(c) $a = 1.42$ (d) $a = 1.65$

Figure 5: (a) Bifurcation diagram for the region $a \in [1, 2]$,(b, c, d)=$(1, 4, 36.5)$ with the initial conditions X_1 (Blue) and X_2 (Red), (b) Coexisting chaotic attractors, (c) Coexisting chaotic attractors, and (d) Coexisting periodic attractors for the new system (2).

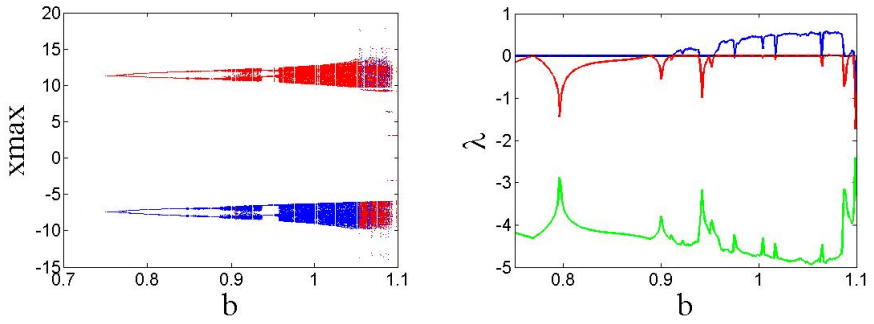

(a) Bifurcation diagram (b) Lyapunov exponent plot

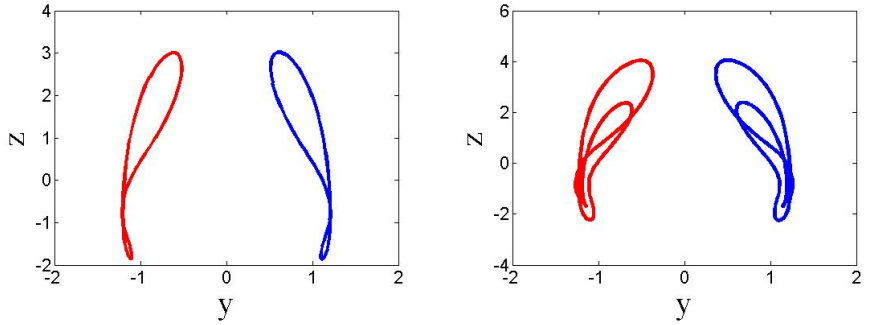

(c) $b = 0.76$ (d) $b = 0.85$

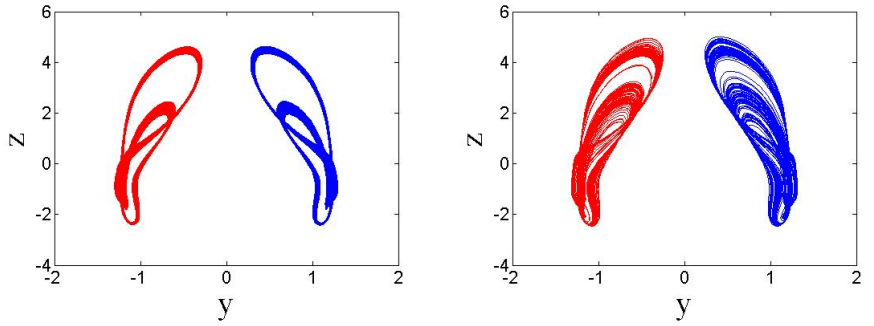

(e) $b = 0.92$ (f) $b = 0.96$

Figure 6: (a) Bifurcation diagram under the parameter $b \in [0.75, 1.1]$ with initial conditions X_1 (Blue) and X_2 (Red). (b) The corresponding Lyapunov exponent plot. (c) Coexisting periodic attractors, (d) Coexisting periodic attractors, (e) Coexisting periodic attractors and (f) Coexisting chaotic attractors when (a, c, d)=$(1.3, 4, 36.5)$ for the new system (2).

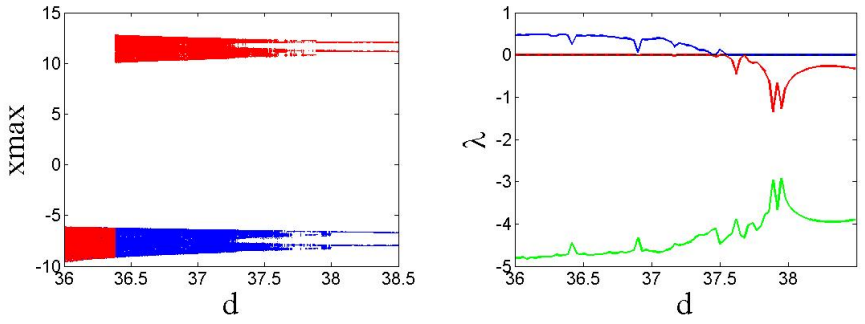

(a) Bifurcation diagram (b) Lyapunov exponent plot

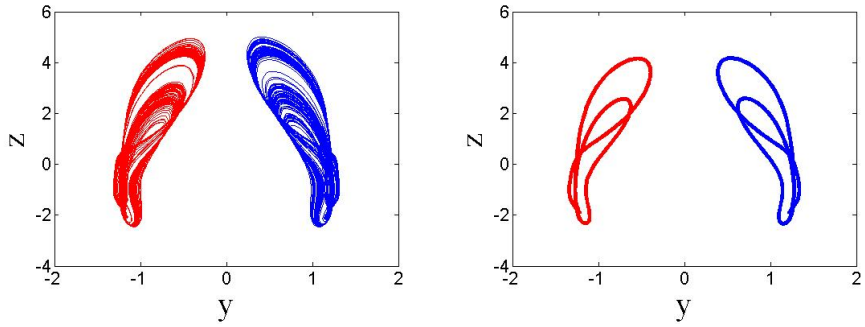

(c) $d = 36.5$ (d) $d = 38.5$

Figure 7: (a) Bifurcation diagram and (b) Lyapunov exponents plot under the parameter $d \in [36, 38.5]$ with X_1 (Blue) and X_2 (Red), (c) Coexisting chaotic attractors, (d) Coexisting periodic attractors when (a, b, c)=$(1.3, 1, 4)$ for the new system (2).

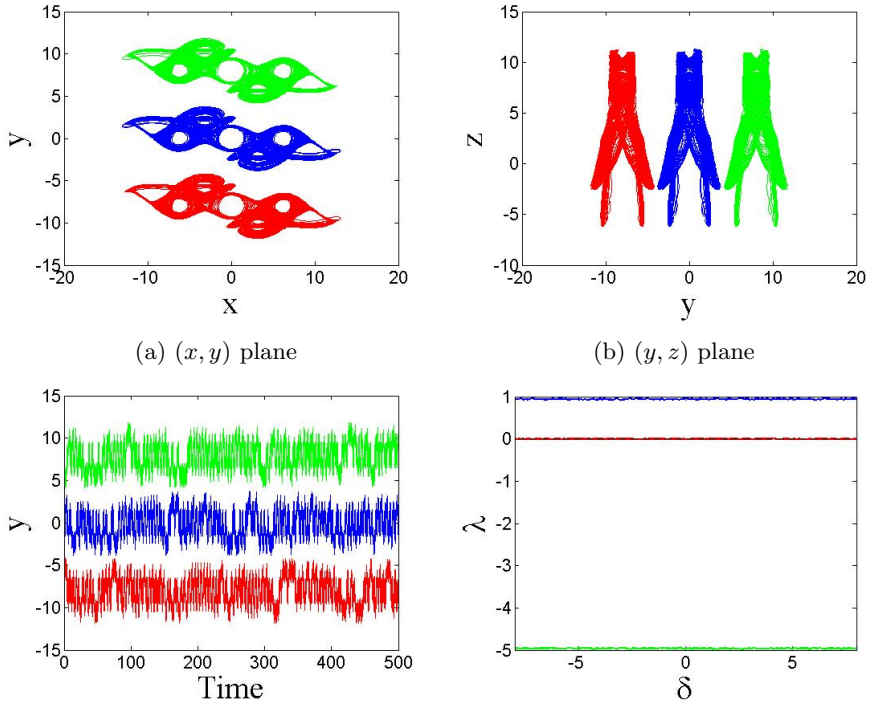

(a) (x, y) plane

(b) (y, z) plane

(c) Time variation of shifted signal y

(d) Lyapunov exponent plot

Figure 8: Parameter oriented infinitely many coexisting attractors when (a, b, c, d)=(1.5.10, 4, 36.5). (a-b) Offset boosted attractors in xy plane and yz plane at δ=0 (Blue),δ=8 (Red) and δ=-8 (Green), (c) Time variation of offset boosted signal y, (d) Constant Lyapunov exponent plot of system (17) in the region $\delta \in [-8, 8]$.

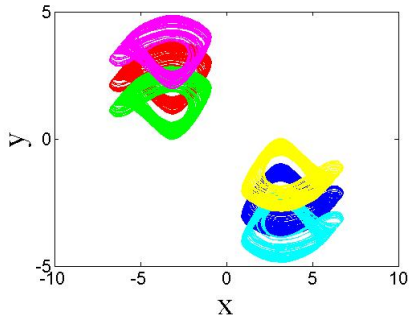

(a) xy plane

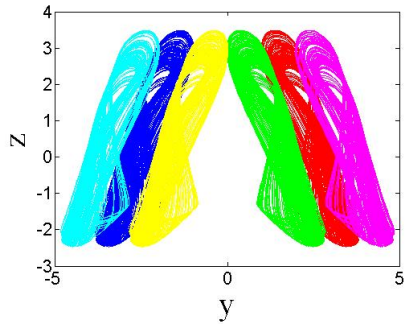

(b) yz plane

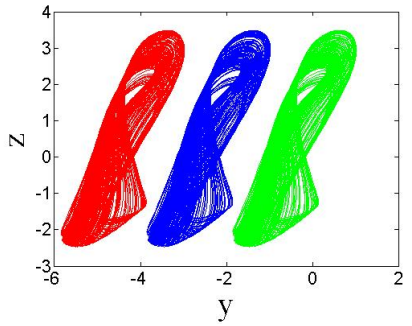

(c) Offset boosted attractors

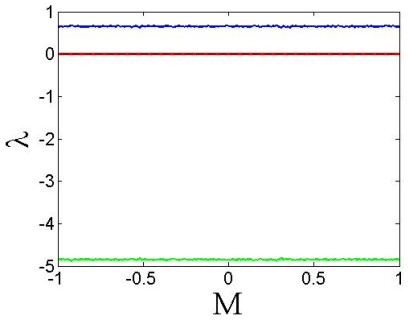

(d) Lyapunov exponent plot

Figure 9: Evolution of offset boosting with multistability when (a, b, c, d)=$(2.5, 10, 4, 36.5)$. (a-b) The offset boosting with initial condition oriented coexisting attractors in xy and yz plane respectively. Note that the distance between the coexisting attractors can be controlled by the offset booster parameter. (c) The offset boosted attractors without initial condition oriented coexisting attractors where $\delta = 0$ (Blue), $\delta = 2$ (Red) and $\delta = -2$ (Green), (d) Lyapnnov exponent plot of system (17) under the booster parameter δ.

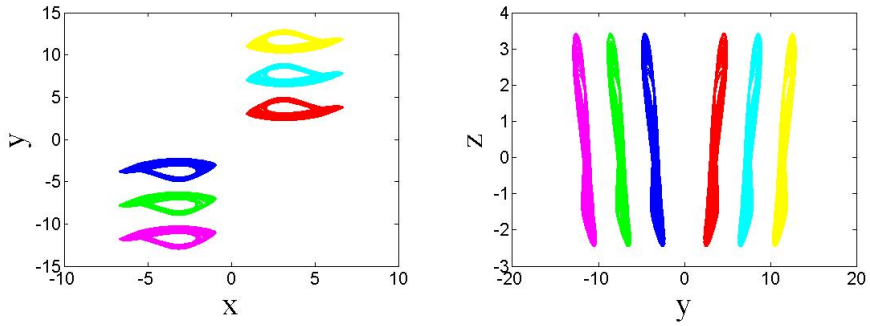

(a) (x, y) plane

(b) (y, z) plane

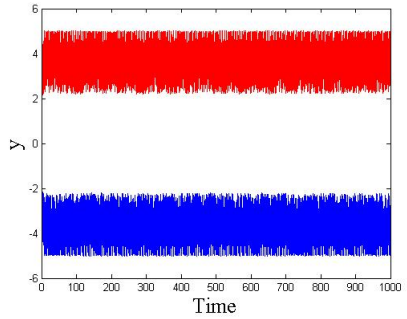

(c) Offset boosted y signal

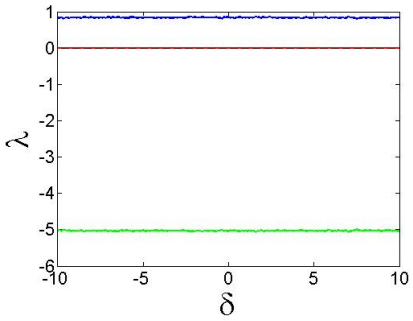

(d) Lyapunov spectrum plot

Figure 10: Evolution of offset boosting with polarity reversal when (a, b, c, d)=$(2.6, 10, 4, 36.5)$. (a) Polarity reversed attractors, (b) Polarity reversed attractors, (c) Shifted signal y, (d) Lyapunov spectrum plot of system (17) under the parameter δ.

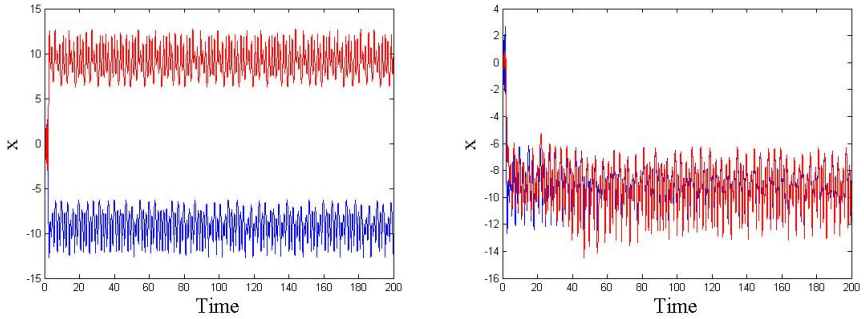

(a) x signal

(b) x signal

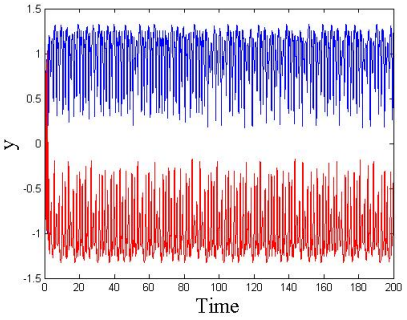

(c) y signal

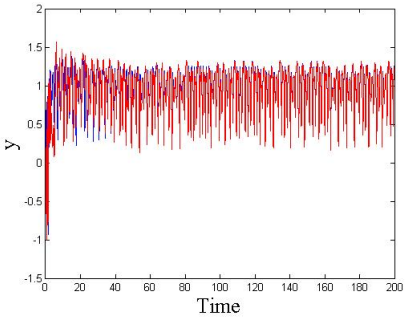

(d) y signal

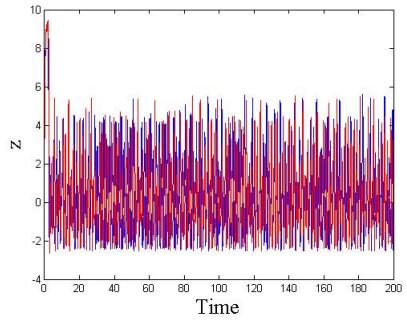

(e) z signal

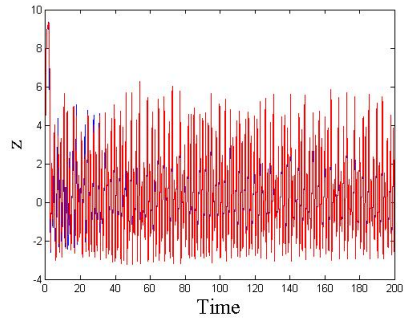

(f) z signal

Figure 11: (a),(c),(e) Unsynchronized state variables and (b),(d),(f) Synchronized state variables between the master system (19) and slave system (20).

Table 1: Different Cases of Parameters in the proposed system

Case	**Parameters**	**Figures**	**Special Features**
1	$a = 1.1$,$b = 1$	Figures 1a & 2a	Two wings attractor
2	$a = 1.3$,$b = 1$	Figures 1b & 2b	Initial condition oriented Coexisting attractors
3	$a = 1.5$,$b = 1$	Figures 1c & 2c	One scroll attractor
4	$a = 1.5$,$b = 10$	Figures 1d & 2d	Seven-scroll attractors in (x, y) plane and offset boosting based coexisting attractors
5	$a = 2.5$,$b = 10$	Figures 1e & 2e	Simultaneous initial condition oriented and offset boosting oriented infinitely many coexisting attractors
6	$a = 2.6$,$b = 10$	Figures 1f & 2f	Polarity reversal and parameter oriented infinitely many coexisting attractors

Table 2: Lyapuov Exponents and Lyapunov Dimensions

Cases	**Lyapunov Exponents**	D_L	l_T	**Types**
1	$l_1 = 0.3985$,$l_2 = 0$, $l_3 = -4.799$	2.083	-4.4005	Dissipative
2	$l_1 = 0.4456$, $l_2 = 0$, $l_3 = -4.7245$	2.094	-4.2789	Dissipative
3	$l_1 = 0.3417$, $l_2 = 0$, $l_3 = -4.438$	2.077	-4.096	Dissipative
4	$l_1 = 0.95127$, $l_2 = 0$, $l_3 = -4.973$	2.1913	-4.0217	Dissipative
5	$l_1 = 0.66232$, $l_2 = 0$, $l_3 = -4.8642$	2.136	-4.2017	Dissipative
6	$l_1 = 0.82392$, $l_2 = 0$, $l_3 = -5.0237$	2.164	-4.1998	Dissipative

Table 3: Equilibrium Points when $\sin x \neq 0$ (Case B) and their corresponding Eigen Values

Case	**Equilibrium Points** (x, y, z)	**Eigen Values**
1	(38.95, -0.26, -1)	(-12.056, 8.018, 0.893)
2	$(\pm 33.35, \mp 0.304, -1)$	(-10.732, 6.6678, 1.1507)
	$(\pm 32.68, \mp 0.31, -1)$	(-10.568, 6.499, 1.1632)
3	$(\pm 33.63, \mp 0.301, -1)$	(-10.8004,6.733, 1.3178)
	$(\pm 32.4, \mp 0.3125, -1)$	(-10.503, 6.426, 1.343)
4	$(-1158.79, 0.0165, -10)$	(-47.31, 43.306, -1.345)
5	$(-578.61, 0.033, -10)$	(2.124, 33.01,-37.05)
6	$(465.64, -0.041, -10)$	(-0.696, 40.39,-44.4)